doi: 10.3969/j.issn.0490-6756.2017.04.017

原子尺度下摩擦的失稳和耗散动力学

李健文[1,2], 刘念华[1]
(1. 南昌大学高等研究院, 南昌 330031; 2. 南昌工程学院理学院, 南昌 330099)

摘　要: 采用 Frenkel-Kontorova 模型和基于双质量双弹簧模型的等效耦合振子模型求解了探针与基底间几种不同耦合类型的能量耗散动力学问题. 发现了纳米尺度下能量耗散失稳现象, 并通过平均耗散功率和粒子相对于质心的位移分析了正弦势和多阱周期性基底势两种情况下的能量耗散特性. 计算结果与最近采用摩擦力显微镜观察的实验结果进行了比较.

关键词: 纳米摩擦; 耗散; 失稳; 摩擦力显微镜
中图分类号: TB34　　**文献标识码**: A　　**文章编号**: 0490-6756(2017)04-0764-07

Instability and dissipation dynamics in atomic scale friction

LI Jian-Wen[1,2], *LIU Nian-Hua*[1]
(1. Institute for Advanced Study, Nanchang University, Nanchang 330031, China;
2. School of Science, Nanchang Institute of Technology, Nanchang 330099, China)

Abstract: Using two different methods, Frenkel-Kontorova (FK) model and equivalent coupled-oscillator model based on two-mass-two-spring model, we solve the dynamics of energy dissipation for several types of coupling between the tip and the substrate. We find the unstable energy dissipation phenomenon on the nanoscale and present a microscopic analysis of properties of energy dissipation via average power dissipated and displacement of the particles relative to the center of mass for sinusoidal potential as well as multiple-well periodic substrate potentials. The results are compared with the observations in recent experiments based on friction force microscope (FFM).

Keywords: Nano-friction; Dissipation; Instability; Friction force microscope

1　Introduction

Understanding friction is among few priorities in nanoscience, where friction has to be controlled at a nanoscale. Due to the fast progress of scanning probe microscopy and computational techniques, experimental and theoretical investigations of friction have experienced an extraordinary development[1-4]. The concepts of wearless sliding, superlubricity and friction control are now successfully attainable and decipherable down to the atomic level[5-7]. Several theoretical investigations based on simple models and atomic simulations revealed various physical phenomena, such as the stick-slip process, thermolubricity, structural phase transitions, etc[8-13]. Furthermore, a significant amount of research efforts have been devoted to reveal the mechanism of

收稿日期: 2015-12-24
基金项目: 973 计划项目(2013CB934200); 国家自然科学基金重点项目 (10832005); 国家自然科学基金(11264030)
作者简介: 李健文(1976－), 男, 江西安远人, 博士研究生, 主要研究领域为纳米表面科学与工程. E-mail: nitljw624@nit.edu.cn
通讯作者: 刘念华. E-mail: nhliu@ncu.edu.cn

nano-friction, which is the most important not only to understand friction but also to develope micro- and nanoelectromechanical devices[14-16]. The core issue is to ascertain how the kinetic energy of sliding contacts converts into heat. The difficulty results from the remarkable complexity found at the sliding interface, making an identification of the fundamental mechanisms involved in friction elusive. Recently several fundamental mechanisms of energy dissipation in friction, i. e., electronic contributions and phononic contributions, have been presented, which deal with this challenge properly[17,18]. These researches have illustrated how friction changes upon an exclusive variation of the electronic and vibrational properties of a surface, respectively.

A quantitative analysis of the energy dissipation, however, has remained several major issues to be resolved. For one thing, the onset of sliding friction and resonant energy transfer in one-dimensional models, such as the Frenkel-Kontorova (FK) chain[9] and the Fermi-Pasta-Ulam lattice[19], have also attracted much recent attention[20-22]. Resonant coupling leading to wide instability windows is found to be responsible for energy dissipation in systems with a quasi-continuous excitation spectrum. Nevertheless, much remains to be understood with regard to dynamic energy transfer channels in the superlubric sliding, such as the effect of interactions between particles of one-dimensional chain on the energy dissipation. To this end, we perform numerical computation with FK model which is useful for studying the relative motion of particles. An interesting phenomenon, that the displacements of the most neighbouring particles relative to the mass center are approximately equal, is found. The novel unstable phenomena and its underlying mechanism report should stimulate further experimental and theoretical interest in achieving persistent superlubricity for further nanomechanical devices. For another, the possible role of velocity in friction appears experimentally and theoretically. As was shown in a study by Quanshui Zheng and co-workers, velocity range can play an important role in the motion of the tip along the surface[23]. One objective of our work is to develop an equivalent coupled-oscillator model, by which we can incorporate the average power dissipated of sliding friction into the quantitative study, basing on the two-mass-two-spring model corresponding to friction force microscope (FFM) measuring system[13]. We have observed a peak of energy dissipation appearing at a well-defined tip velocity of the order of approximately 0.1-1 m/s and interpreted Zheng's experimental results accordingly.

The organization of the paper is as follows. In Sec. 2 we briefly describe the theoretical model and methods. Sec. 3 is devoted to the presentation of the simulation results concerning instability and power dissipation. Conclusions are given in the last section.

2 Theoretical approach

2.1 FK model

In its simplest form, the standard FK model describes the interaction of a one-dimensional chain of particles with a rigid, modulated substrate potential. Particles within the chain interact via a nearest-neighbor harmonic potential. Some important generalizations of the FK model have already been considered by studying more general types of substrate potential[24], as well as anharmonic interactions which may vary substantially from the regular one assumed in the standard FK model[25].

In this paper, we consider the FK model consists of a harmonic linear chain of particles of mass m_0 with period a_0. The spring constant between the particles is κ. The model can be enriched by considering the dynamics of the particles. We include the kinetic energy of the particles by defining $\tau = t/\tau_0$, where t is the time and $\tau_0 = \sqrt{m_0/\kappa}$. We express all energies in units of $E_0 = \kappa a_0^2$, times in units of τ_0 and lengths in units of a_0.

For an external sinusoidal periodic potential

with period a_s and amplitude $U_0/2\pi$, the resulting equation of motion can be written as

$$\frac{d^2\mu_i}{d\tau^2} = (\mu_{i+1} + \mu_{i-1} - 2\mu_i) + \frac{\lambda}{a_s}\sin\frac{2\pi\mu_i}{a_s} - \tilde{\gamma}\frac{d\mu_i}{d\tau} \quad (1)$$

where $\mu_i = u_i/a_0$ is the position of particle i of the chain representing a sliding body. $\tilde{a}_s = a_s/a_0$ is the ratio between the period of the external potential and the unextended equilibrium length of the chain. This ratio can be a rational number and the situation is called commensurate, or the ratio is an irrational number and the situation is called incommensurate. $\tilde{\gamma} = \gamma\tau_0$ is the friction constant. The depth of the external potential is depicted by $\lambda = U_0/E_0$, which gives an estimate of the dominant term in the potential energy.

For a multiple-well periodic substrate, we consider the following equations of motion

$$\frac{d^2\mu_i}{d\tau^2} = (\mu_{i+1} + \mu_{i-1} - 2\mu_i) + \frac{\lambda}{\tilde{a}_s}\left(\sin\frac{2\pi\mu_i}{\tilde{a}_s} + \sin\frac{2\pi\beta\mu_i}{\tilde{a}_s}\right) - \tilde{\gamma}\frac{d\mu_i}{d\tau} \quad (2)$$

The two lengths $\tilde{a}_s$ and $\tilde{c} = \tilde{a}_s/\beta$ of the substrate potential are chosen to be mutually commensurate, i. e., $\tilde{a}_s/\tilde{c} = M_1/M_2$, with M_1 and M_2 as integer numbers. This means that the periodicity of the substrate turns out to be $T = M_2\tilde{a}_s = M_1\tilde{c}$.

To study the dynamics of the system, we solve the equations of motion numerically by using the Verlet velocity algorithm with a step of $\tau_0/10^5$ and calculate the positions of the particles, the position $Q = (1/N)\sum_{i=1}^{N}\mu_i$ and velocity $P = (1/N)\sum_{i=1}^{N}\frac{d\mu_i}{d\tau}$ of the centre of mass (CM).

2.2 Equivalent coupled-oscillator model

In general, the two-mass-two-spring model describing FFM measuring system is demonstrated using two coupled Langevin-type equations of motion[26,27], one for the cantilever and tip combination with coordinate X as well as mass M, and the other for the tip apex with coordinate x and effective mass m moving with respect to X. For a one-dimensional geometry and a sinusoidal apex-surface interaction, $U_s = (U_0/2)[1 - \cos(2\pi x/a)]$, with the amplitude of the potential corrugation U_0 and the substrate lattice period a. To investigate the power dissipation of the system, an equivalent coupled-oscillator model is developed, as shown in Fig. 1. Action that the substrate surface imposes on the tip apex can be substituted by a periodical driving force. The dynamical behavior of the system is governed by the equivalent coupled Langevin equations:

$$M\frac{d^2}{dt^2}X = -KX + k(x - X) - M\gamma_M\frac{d}{dt}X + R_M(t) \quad (3)$$

$$m\frac{d^2}{dt^2}x = -k(x - X) - m\gamma_m\frac{d}{dt}x + R_m(t) + F(t) \quad (4)$$

Here, Eq. (3) describes the motion of the cantilever, and Eq. (4) describes the motion of the tip apex; K and k denote the stiffness of the cantilever and of the tip apex, respectively; $F(t)$ is periodic driving force. $R_M(t)$ and $R_m(t)$ are white noises satisfying the fluctuation-dissipation relations $\langle R_M(t_1)R_M(t_2)\rangle = 2M\gamma_M k_B T\delta(t_1 - t_2)$ and $\langle R_m(t_1)R_m(t_2)\rangle = 2m\gamma_m k_B T\delta(t_1 - t_2)$.

In order to study the response of the coupled-oscillator to the Fourier component of driving force, the noise has been artificially switched off completely. Let's drive the syetem with a force $F(t) = F_0\exp(-i\omega t)$ of specific frequency $\omega = 2\pi V/a$, where V is the velocity of the support corresponding to the two-mass-two-spring model. The solutions of Fourier component of displacements can be written as $X = X_0\exp(-i\omega t)$ and $x = x_0\exp(-i\omega t)$. We plug them into Eqs. (3) and (4) to get

$$-M\omega^2X_0 + KX_0 + kX_0 - kx_0 - i\omega M\gamma_M X_0 = 0 \quad (5)$$

$$-m\omega^2x_0 + kx_0 - kX_0 - i\omega m\gamma_m x_0 = F_0 \quad (6)$$

We can obtain the frequency-dependent response function

$$\tilde{\chi}(\omega)=\frac{1}{m\omega_m^2}\left[\frac{\frac{\omega^2}{\omega_m^2}-(\sigma+\beta)+i\frac{\omega}{\omega_m}\frac{\gamma_M}{\omega_m}}{\{(1-\frac{\omega^2}{\omega_m^2})[\frac{\omega^2}{\omega_m^2}-(\sigma+\beta)]+(\frac{\omega^2}{\omega_m^2})(\frac{\gamma_M\gamma_m}{\omega_m^2})+\beta\}+i\frac{\omega}{\omega_m}\{\frac{\gamma_M}{\omega_m}(1-\frac{\omega^2}{\omega_m^2})-\frac{\gamma_m}{\omega_m}[\frac{\omega^2}{\omega_m^2}-(\sigma+\beta)]\}}\right] \tag{7}$$

where

$$\omega_M=\sqrt{\frac{K}{M}},\omega_m=\sqrt{\frac{k}{m}},\beta=\frac{m}{M},\sigma=\left(\frac{\omega_M}{\omega_m}\right)^2$$

Since the Fourier transform

$$\chi(t)=\frac{1}{2\pi}\int\tilde{\chi}(\omega)\,e^{i\omega t}d\omega \tag{8}$$

we have

$$x(t)=\int_{-\infty}^{t}\chi(\tau-t)F(\tau)d\tau \tag{9}$$

The power dissipated is

$$P(t)=\frac{dW}{dt}=F(t)\left[\frac{d}{dt}x(t)\right]=F(t)\frac{d}{dt}\int_{-\infty}^{+\infty}\chi(t-t')F(t')dt' \tag{10}$$

Let's drive the system with a force of a specific frequency ω, so that

$$F(t)=F_0\cos(\omega t)=\frac{F_0}{2}(e^{i\omega t}+ie^{-i\omega t}) \tag{11}$$

We can calculate the average power dissipated over a cycle

$$\bar{P}=\frac{1}{T}\int_0^T dtP(t)=\frac{1}{m\omega_m^2}2\omega\left(\frac{F_0}{2}\right)^2\frac{(BC-AD)}{C^2+D^2} \tag{12}$$

where

$$F_0=\frac{\pi U_0}{a},A=\frac{\omega^2}{\omega_m^2}-(\sigma+\beta),B=\frac{\omega}{\omega_m}\frac{\gamma_M}{\omega_m}$$

$$C=(1-\frac{\omega^2}{\omega_m^2})A+(\frac{\omega^2}{\omega_m^2})(\frac{\gamma_M\gamma_m}{\omega_m^2})+\beta$$

$$D=\frac{\omega}{\omega_m}\{\frac{\gamma_M}{\omega_m}(1-\frac{\omega^2}{\omega_m^2})-\frac{\gamma_m}{\omega_m}A\}$$

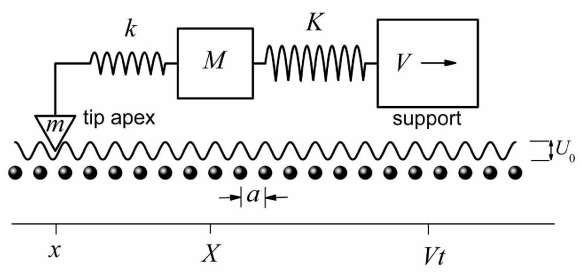

(a)

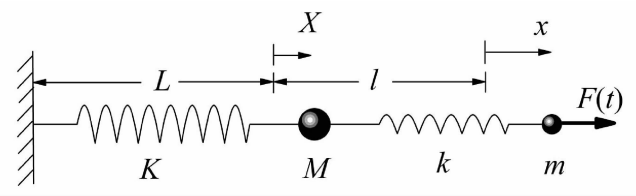

(b)

Fig. 1　(a) Two-mass-two-spring model corresponding to FFM measuring system, and (b) Equivalent coupled-oscillator model. Action that substrate surface imposes on the tip apex is substituted by a periodical driving force $F(t)$, whose frequency is $\omega=2\pi V/a$.

3　Numerical results and discussion

3.1　Instability leading to dissipation

It is attractive to explore in what final state the system will be, after the evolution from a situation where all the particles start with the same velocity. $N=31$ particles are distributed along the one-dimensional chain. All the particles at a time $\tau_0=0$ take a random displacement and get an initial kinetic energy of $0.6E_0$. For the coupling between periodic potential and the chain of particles, we choose $\lambda=1.0$. For each initial state of the system we store data points each $0.01\tau_0$.

We are interested in the dynamic characteristics of the systems. The most important part of results of these simulations for the displacement of particles relative to CM is shown in Fig. 2. Only partial particles are presented for clarity. One can see that, the displacements are almost changeless until particles No6 and No7 adjoin together, which indicates that the system step into an unstable state because of the interaction of the chain of particles with the external periodic potential. At this time, all particles oscillate abruptly and the nearest neighbor particles approach. This sliding back and forth has amplitude of at most half a_0. The kinetic energy decays and the poten-

tial energy increases with time until they approach together, when they also fluctuate strongly, as shown in Fig. 3. These sharp variations in time means that the thermal motions intensify, thus thermal dissipations intensify accordingly. The forward motion of the sliding body as a whole is transformed into internal vibrational motion. We consider that the coupling between the chain and the substrate is the strongest, so the resonance appears, which is a primary source that drains the translational energy and responsible for the sudden drops.

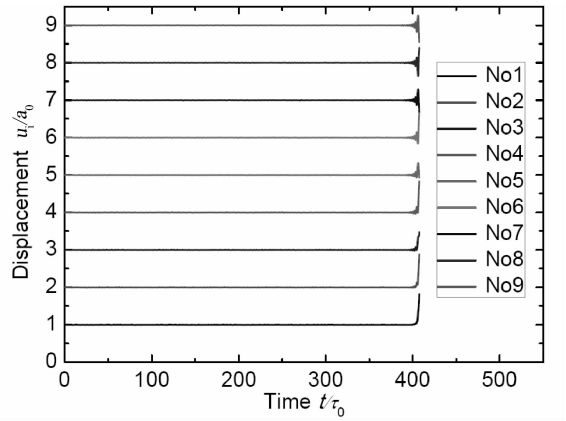

Fig. 2 Displacement of the particles relative to CM as a function of time for a sinusoidal substrate potential. Only a limited portion of the particles is displayed for clarity.

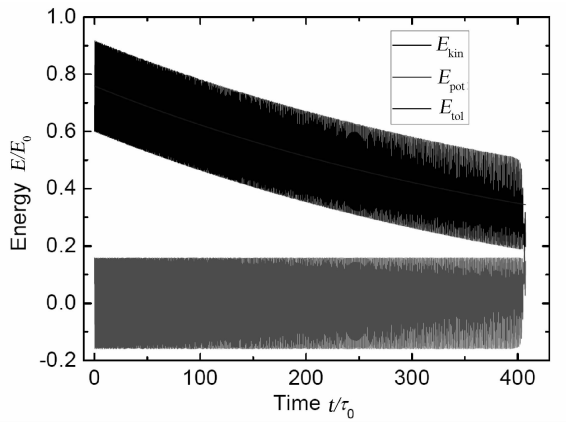

Fig. 3 Energy as a function of time for a sinusoidal substrate potential. E_{kin} is the kinetic energy, E_{pot} is the potential energy, E_{tol} is the total energy. The maximum of time corresponds with that of Fig. 2.

To model real physical systems, we also study the dynamics of a FK chain subject to a substrate potential defined by the sum of two sinusoidal functions with different periodicities. Fig. 4 shows, for the $\beta = 24/30$ and the initial kinetic energy $1.0E_0$, the time evolution of displacement of the partial particles relative to CM for multiple-well periodic substrate potential. We see an oscillatory phase, where the relative displacement aperiodically goes back to the initial value, which is very different from that of a sinusoidal substrate potential. However, after some time the same phenomenon occur, particles No4 and No5 adjoin together. It indicates that the system step into an unstable state because of the interaction of the chain of atoms with the external multiple-well periodic potential. From Fig. 5 we see that the CM kinetic energy has been transformed into the thermal energy and potential energy of the particles of the body.

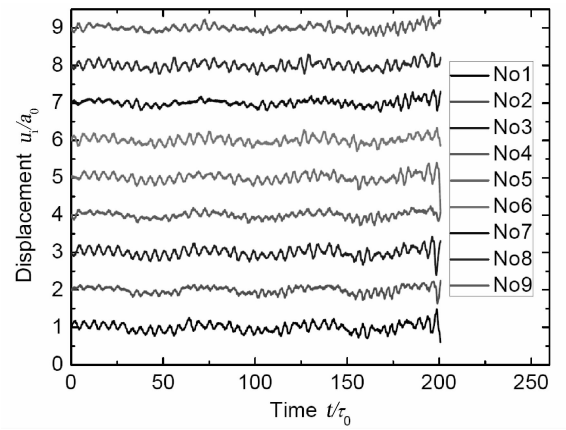

Fig. 4 Displacement of the partial particles relative to CM as a function of time for a multiple-well periodic substrate potential.

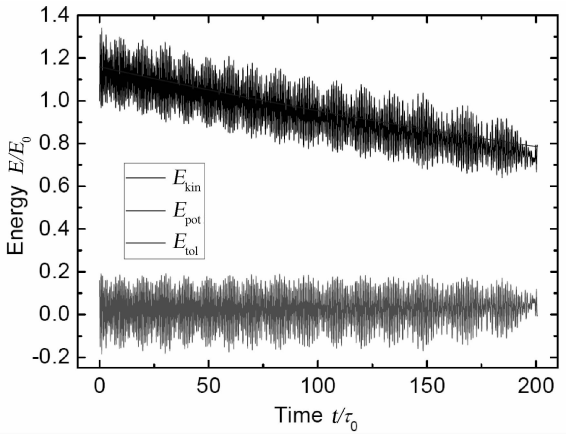

Fig. 5 Energy as a function of time for a multiple-well periodic substrate potential. The maximum of time corresponds with that of Fig. 4.

3.2 Power dissipation

In this section, we apply the equivalent coupled-oscillator model based on the two-mass-two-spring model to analyze the dependence of the energy dissipation on the velocity of support. Calculations have been performed for the system parameters involved: tip stiffness $k = 3$ N/m, substrate lattice spacing $a = 0.25$ nm, the cantilever mass $M = 1 \times 10^{-9}$ kg, and the effective mass of the contact $m = 1 \times 10^{-20}$ kg, as used in Ref. 27. Average power dissipated calculated according to Eq. (12) is shown in Fig. 6 for the cases of relatively hard ($K = 60$ N/m) and soft ($K = 6$ N/m) external springs, which is typical for FFM experiments. The results indicate that a high energy loss is met in a velocity range of approximately 0.1 to 1 m/s, which plays an important role in the motion of the tip along the surface.

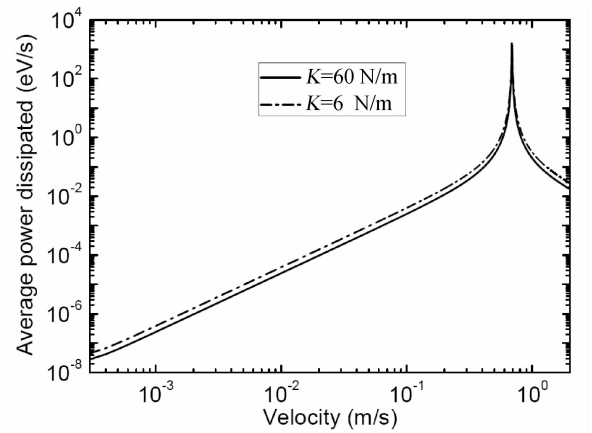

Fig. 6　Average power dissipated as a function of velocity.

Recently nanoscale superlubricity has been studied using FFM and microtip manipulation at sliding speeds below 10 μm/s[5,28,29]. Furthermore, microscale superlubricity was first observed in the self-retracting motion (SRM) of microscopic graphite flake that retracts spontaneously back onto the mesa after being sheared from micron sized mesas fabricated on highly oriented pyrolytic graphite to minimize interfacial energy[30,31]. Zheng *et al*. reported first measurements of the highly reproducible SRM speeds from 10^{-4} m/s to 24 m/s over a wide range of temperatures. Especially the SRM speeds range approximately from 10^{-4} m/s to 1 m/s around room temperatures (see Fig. 2 and Fig. 3 in Ref. 23). It is of importance to understand the reason that the retracting flake accelerates to the order of magnitude. For $k = 3$ N/m, the frequency of the apex bending vibrations $\omega_m = 1.732 \times 10^{10}\,\mathrm{s}^{-1}$. According to $\omega/\omega_m = 2\pi V/a\omega_m = 1.45$ V, we find $V = 0.698\omega/\omega_m$. When the frequency of driving force is equal to the eigen frequency of the coupled−oscillator, the sliding speed is 0.698 m/s. As a result, a resonance coupling of a slider to a collective phase occurs. The energy dissipation approaches the maximum. Our calculations present a good accordance with the experiments' results of Zheng *et al*.

Furthermore, the width of the peak for the cases of relatively hard external spring has little increase relative to that of soft external spring. It should be noted that there is no selective absorption relating to the frequency for the white noises because its Fourier component is constant.

4 Conclusions

In summary, we analyze the fundamental processes in friction and energy dissipation using two different methods of both technological relevance and physical fascination from a nanostructure coupled to a substrate. Here, emphasis is placed on energy dissipation between the particles of the chain, and the energy transfer through interface between the nanoparticles and the substrate. We also develop a model based on the two-mass-two-spring model to study the dissipation of energy adsorbates into a substrate. The results fit well to the experiments, and the theory shows a clear picture of energy dissipation through average power, and allows quantitative analysis on the atomic scale. Studies of the energy dissipation will contribute to understanding general friction phenomena and to the development of nanotribology.

References:

[1]　Urbakh M, Meyer E. The renaissance of friction

[J]. Nature Mater, 2010, 9: 8.

[2] Stone T W, Horstemeyer M F. Length scale effects of friction in particle compacting using atomistic simulations and a friction scaling model [J]. J Nanopart Res, 2012, 14: 1121.

[3] Langer M, Kisiel M, Pawlak R, *et al*. Giant frictional dissipation peaks and charge-density-wave slips at the $NbSe_2$ surface [J]. Nature Mater, 2014, 13: 173.

[4] Liu Z, Wang W, Liu L. Comparative study on friction force pattern anisotropy of graphite [J]. Appl Surf Sci, 2015, 332: 473.

[5] Dienwiebel M, Verhoeven G S, Pradeep N, *et al*. Superlubricity of graphite [J]. Phys Rev Lett, 2004, 92: 126101.

[6] Socoliuc A, Gnecco E, Maier S, *et al*. Atomic-scale control of friction by actuation of nanometer-sized contacts [J]. Science, 2006, 313: 207.

[7] Ma M, Benassi A, Vanossi A, *et al*. Critical length limiting super-low friction [J]. Phys Rev Lett, 2015, 114: 055501.

[8] Tomlinson G A. CVI. A molecular theory of friction [J]. Philos Mag, 1929, 7: 905.

[9] Frenkel J, Kontorova T. On the theory of plastic deformation and twinning [J]. Phys Z Sowjetunion, 1938, 13: 1.

[10] Hirano M. Atomistics of friction [J]. Surf Sci Rep, 2006, 60: 159.

[11] Zhong W, Tománek D. First-principles theory of atomic-scale friction [J]. Phys Rev Lett, 1990, 64: 3054.

[12] Buldum A, Ciraci S. Atomic-scale study of dry sliding friction [J]. Phys Rev B, 1997, 55: 2606.

[13] Krylov S Y, Frenken J W M. Thermal contact delocalization in atomic scale friction: a multitude of friction regimes [J]. New J Phys, 2007, 9: 398.

[14] Dias R A, Rapini M, Costa B V, *et al*. Temperature dependent molecular dynamic simulation of friction [J]. Braz J Phys, 2006, 36: 741.

[15] Socoliuc A, Bennewitz R, Gnecco E, *et al*. Transition from stick-slip to continuous sliding in atomic friction: entering a new regime of ultralow friction [J]. Phys Rev Lett, 2004, 92: 134301.

[16] Filleter T, McChesney J L, Bostwick A, *et al*. Friction and dissipation in epitaxial graphene films [J]. Phys Rev Lett, 2009, 102: 086102.

[17] Park J Y, Ogletree D F, Thiel P A, *et al*. Electronic control of friction in silicon pn junctions [J]. Science, 2006, 313: 186.

[18] Cannara R J, Brukman M J, Cimatu K, *et al*. Nanoscale friction varied by isotopic shifting of surface vibrational frequencies [J]. Science, 2007, 318: 780.

[19] Fermi E, Pasta J, Ulam S. Studies of non-linear problems [M]. Chicago: University of Chicago, 1965.

[20] Consoli L, Knops H J F, Fasolino A. Onset of friction in incommensurate systems [J]. Phys Rev Lett, 2000, 85: 302.

[21] Strunz T, Elmer F J. Driven Frenkel-Kontorova model I [J]. Phys Rev E, 1998, 58: 1601.

[22] Christie G, Henry B I. Resonance energy transfer in the induction phenomenon in quartic Fermi-Pasta-Ulam chains [J]. Phys Rev E, 1998, 58: 3045.

[23] Yang J, Liu Z, Grey F, *et al*. Observation of high-speed microscale superlubricity in graphite [J]. Phys Rev Lett, 2013, 110: 255504.

[24] van der Ende J A, de Wijn A S, Fasolino A. The effect of temperature and velocity on superlubricity [J]. J Phys: Condens Matter, 2012, 24: 445009.

[25] Vanossi A, Röder J, Bishop A R, *et al*. Driven, underdamped Frenkel-Kontorova model on a quasiperiodic substrate [J]. Phys Rev E, 2000, 63: 017203.

[26] Abel D G, Krylov S Y, Frenken J W M. Evidence for contact delocalization in atomic scale friction [J]. Phys Rev Lett, 2007, 99: 166102.

[27] Krylov S Y, Frenken J W M. The crucial role of temperature in atomic scale friction [J]. J Phys: Condens Matter, 2008, 20: 354003.

[28] Kis A, Jensen K, Aloni S, *et al*. Interlayer forces and ultralow sliding friction in multiwalled carbon nanotubes [J]. Phys Rev Lett, 2006, 97: 025501.

[29] Dietzel D, Ritter C, Mönninghoff T, *et al*. Frictional duality observed during nanoparticle sliding [J]. Phys Rev Lett, 2008, 101: 125505.

[30] Zheng Q, Jiang B, Liu S, *et al*. Self-retracting motion of graphite microflakes [J]. Phys Rev Lett, 2008, 100: 067205.

[31] Liu Z, Yang J, Grey F, *et al*. Observation of microscale superlubricity in graphite [J]. Phys Rev Lett, 2012, 108: 205503.